

Electronic Supplementary Information

Cyclotrimerization of alkynes catalyzed by a self-supported cyclic trinuclear nickel(0) complex with α -diimine ligands

Lingyi Shen,^a Yanxia Zhao,^a Qiong Luo,^b Qian-Shu Li,^b Bin Liu,^a Carl Redshaw,^{a,c} Biao Wu,^a Xiao-Juan Yang^{*a}

^a Key Laboratory of Synthetic and Natural Functional Molecule Chemistry of the Ministry of Education, College of Chemistry and Materials Science, Northwest University, Xi'an 710069, China

^b Center for Computational Quantum Chemistry, South China Normal University, Guangzhou 510631, China

^c School of Mathematics & Physical Sciences, University of Hull, Cottingham Road, Hull, HU6 7RX, UK

Table of contents:

S1. Experimental Section

S1.1 General considerations

S1.2 X-ray Crystal Structure Determination

S1.3 Synthesis and characterization of the cyclotrimerization products

S1.4 Kinetics study

S2. DFT Computations

S1. Experimental Section

S1.1 General considerations

All reactions and manipulations of air- and moisture-sensitive compounds were carried out under argon or nitrogen by using standard Schlenk or dry box techniques. The solvents Et₂O, DME, toluene and THF were dried by Na and were distilled under nitrogen. CH₂Cl₂, CH₃CN and DMF were dried using CaH₂ and were distilled under nitrogen. Benzene-*d*₆ was dried over Na/K alloy. Dimethoxyethane nickel dibromide [(DME)NiBr₂]^{1a} and the ligand L^{Me-2,4}^{1b} were prepared according to literature procedures. Sodium metal, anhydrous nickel dibromide and alkynes were purchased from Alfa Aesar. NMR spectra were recorded on a Bruker Avance-400 MHz spectrometer in benzene-*d*₆ and CDCl₃.

Magnetic properties of complex **1**, [Ni₃(μ₂-Br)₃(μ₃-Br)₂(L^{Me-2,4})₃] Br

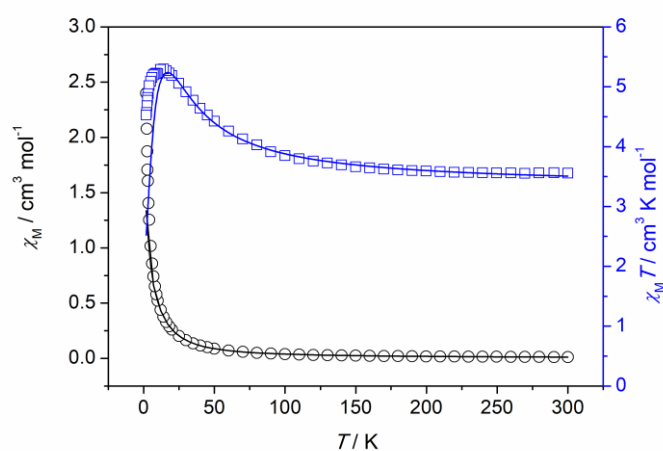


Fig. S1. Plots of χ_M vs. T and $\chi_M T$ vs. T for complex **1** in the temperature range of 2–300 K. The solid lines are the fitting results.

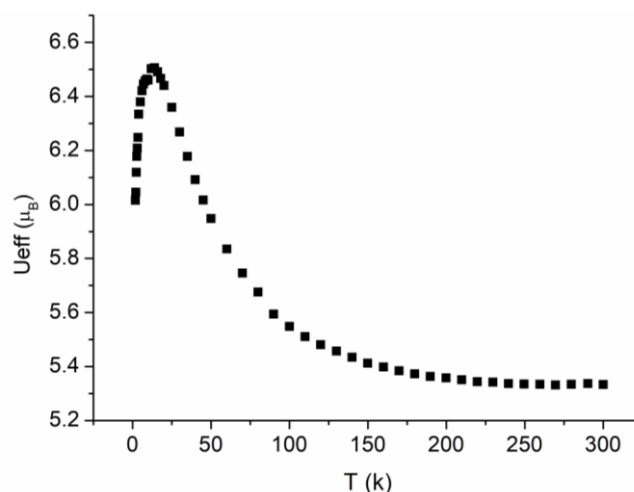


Fig. S2. Temperature dependence of the effective magnetic moment of **1**.

Variable-temperature magnetic susceptibilities for **1** were measured in the temperature range 2–300 K under a constant magnetic field of 1000 Oe. The plots of $\chi_M T$ versus T are shown in Fig. S2. Upon cooling, the $\chi_M T$ steadily increases from 3.56 cm³ K mol⁻¹ at 300 K to 4.02 cm³ K mol⁻¹ at 80 K. Below this

temperature, $\chi_M T$ sharply increases to reach a maximum of $5.29 \text{ cm}^3 \text{ K mol}^{-1}$ at 14 K, which indicates the presence of the intramolecular ferromagnetic coupling between adjacent Ni^{2+} centers.² The value of $\chi_M T$ drops sharply below 14 K, which might be attributed to the weak intermolecular antiferromagnetic interactions and/or the zero-field-splitting (ZFS) effects in the ground state.³

At such conditions, the magnetic interactions within the $\{\text{Ni}_3\}$ cluster can be defined according to the following isotropic spin Hamiltonian:

$$\hat{H} = -2J(\hat{S}_1\hat{S}_2 + \hat{S}_2\hat{S}_3 + \hat{S}_3\hat{S}_1) \quad (1)$$

where the J represents the coupling constant between adjacent Ni^{2+} centers. Taking the above isotropic spin Hamiltonian and molecular field approximation, we have fitted the magnetic susceptibility data with the following eq.

$$\chi_M = \frac{2Ng^2\beta^2}{kT} \times \frac{3e^{2J/kT} + 10e^{6J/kT} + 14e^{12J/kT}}{1 + 9e^{2J/kT} + 10e^{6J/kT} + 7e^{12J/kT}} \quad (2)$$

$$\chi = \chi_M / [1 - (2zJ/Ng^2\beta^2)\chi_M] \quad (3)$$

The above model gives a good fit of the magnetic properties of complex **1** in the whole temperature range: $g = 2.11$, $J = 4.74 \text{ cm}^{-1}$, $zJ = -0.27 \text{ cm}^{-1}$ and $R = 7.7 \times 10^{-4}$ (the error factor R is defined as $\sum[(\chi_M T)_{\text{obsd}} - (\chi_M T)_{\text{calcd}}]^2 / \sum[(\chi_M T)_{\text{obsd}}]^2$). The positive J value demonstrates the ferromagnetic coupling between Ni^{2+} ions through the bridging Br^- ions.

Moreover, plot of temperature dependence of the effective magnetic moment (μ_{eff}) is shown in Fig. S2. The effective magnetic moment increases slowly from $5.33 \mu_B$ at 300 K to $6.50 \mu_B$ at 14 K.

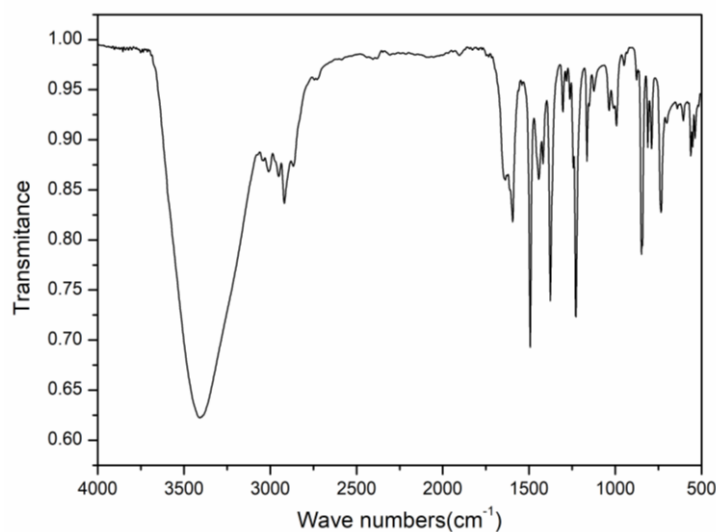


Fig. S3. IR spectrum of complex **1**.

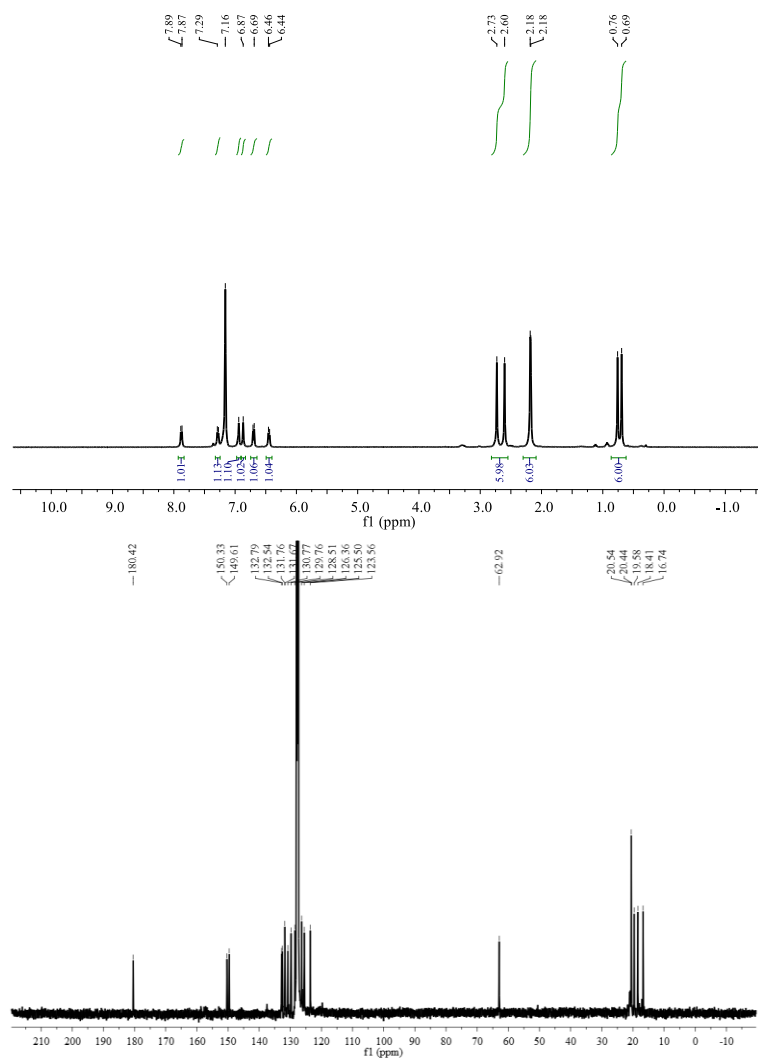


Fig. S4. ¹H and ¹³C NMR spectra of complex **2**.

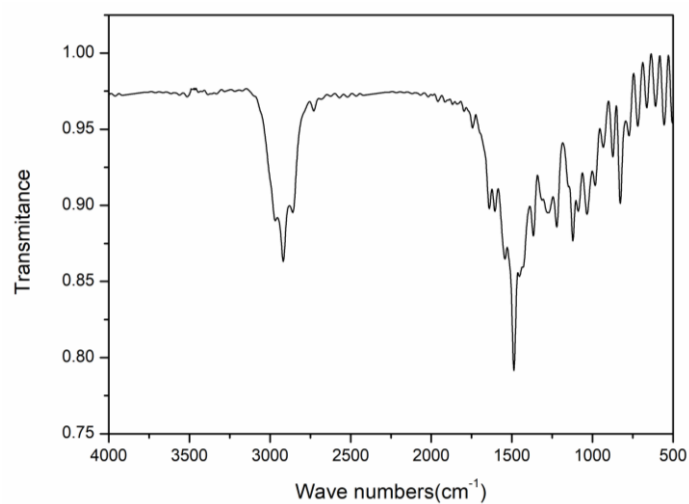


Fig. S5. IR spectrum of complex **2**.

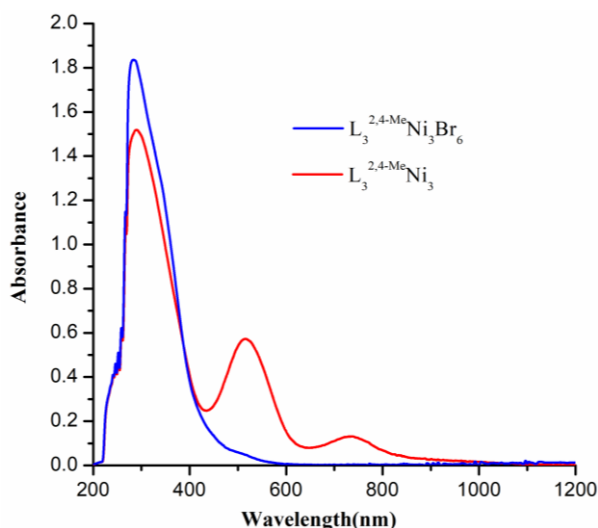


Fig. S6. UV-vis-NIR spectra of **1** ($6.5 \times 10^{-5} \text{ mol L}^{-1}$, red) and **2** ($4.6 \times 10^{-5} \text{ mol L}^{-1}$, blue) in THF.

UV-vis-near IR spectra of complexes **1** and **2** were recorded in THF at room temperature (Fig. S6). The spectra consist of absorptions across the UV, visible and near-IR regions. The absorption spectra of **1** and **2** are similar in the higher-energy region, with dominant peaks at about 289 nm. These absorptions are assigned to ligand-centered (π - π^*) transitions.⁴ However, complex **2** has two additional weak bands at 516 nm and 733 nm, which are expected to be the metal-to-ligand charge-transfer (MLCT) bands.⁵ TD-DFT computations were conducted at the bp86/6-311G* level on complex **2**. Both of the two theoretical bands at 543 and 497 nm correspond to the experimental 516 nm absorption and the lower energy band at 697 nm (experimental 733 nm) corresponds to an excitation from the nickel *d* orbital to the ligands (HOMO-4→LUMO+4, HOMO-3→LUMO+4, HOMO→LUMO+7 and HOMO-3→LUMO+2), indicating the facile transition of the metal-to-ligand charge-transfer under UV-Vis irradiation (Fig. S7).

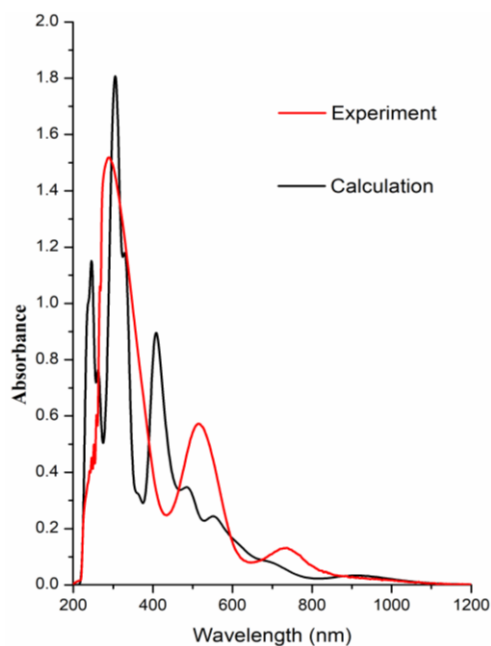


Fig. S7. Comparison of the experimental and computational (bp86/6-311G *) UV/Vis spectra of **2**. (the scale factor is 1.00 and the half-width is 2500 cm^{-1})

Table S1. Absorption wavelengths, oscillator strengths, main transition pairs and amplitudes for selected excited states of complex **2** at the bp86/6-311G * level of theory.

no.	transition (%)	Calculated transition energy/nm	Oscillator strength
1	HOMO-3=>LUMO+2 (72)	697	0.0084
2	HOMO=>LUMO+7 (51)	543	0.0101
3	HOMO-4=>LUMO+4 (39)	497	0.0187
	HOMO-3=>LUMO+4 (39)		

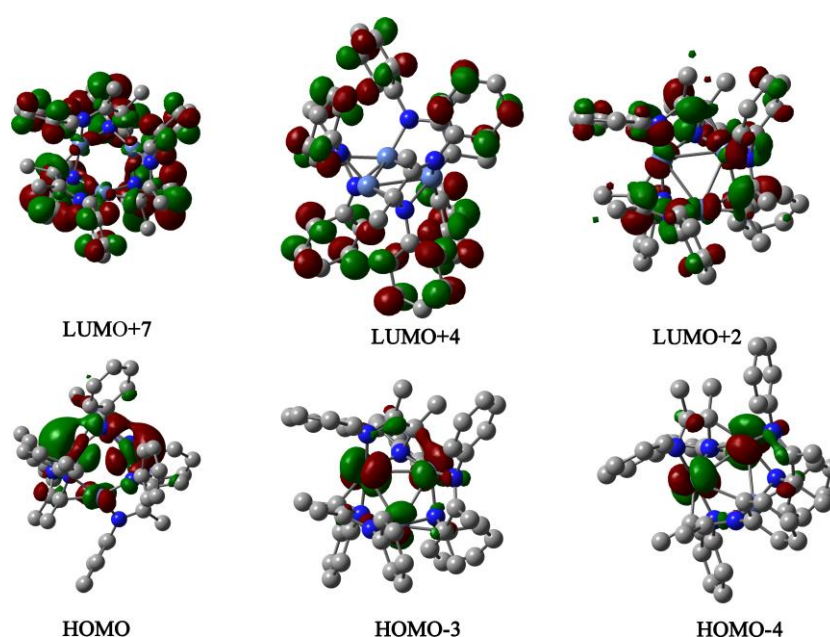


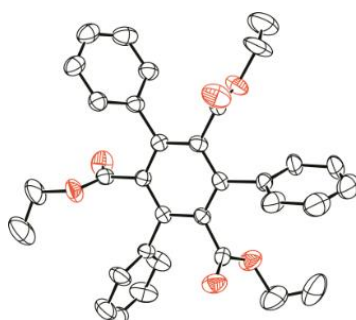
Fig. S8. Molecular orbitals of complex **2**.

S1.2 X-ray crystal structure determination

Diffraction data for the complexes **1** and **2** (sealed in thin glass tubes) and the cyclotrimerization product **4a** were collected on a Bruker SMART APEX II diffractometer at room temperature (298 K) with graphite-monochromated Mo K α radiation ($\lambda = 0.71073$ Å). An empirical absorption correction using SADABS was applied for all data.⁶ The structures were solved by direct methods using the SHELXS program.⁷ All non-hydrogen atoms were refined anisotropically by full-matrix least squares on F^2 by the use of the program SHELXL.⁷ Hydrogen atoms bonded to carbon were included in idealized geometric positions with thermal parameters equivalent to 1.2 times those of the atom to which they were attached. Crystallographic data and refinement details for **1**, **2** and **4a** are given in Table S2.

Table S2. Crystallographic data and refinement details for compounds **1**, **2**, **4a**.

	1	2	4a
formula	C ₆₀ H ₇₂ Br ₆ N ₆ Ni ₃	C ₆₀ H ₇₂ N ₆ Ni ₃	C ₃₃ H ₃₀ O ₆
fw	1532.83	1053.37	522.57
crystal system	Trigonal	Monoclinic	Monoclinic
space group	<i>P</i> -3	<i>P</i> 2(1)/ <i>n</i>	<i>Cc</i>
<i>a</i> /Å	13.198(5)	13.1720(18)	22.007(7)
<i>b</i> /Å	13.198(5)	20.129(3)	12.847(7)
<i>c</i> /Å	23.606(9)	21.285(3)	11.149(5)
<i>a</i> /deg	90	90	90
<i>β</i> /deg	90	103.793(2)	112.394(8)
<i>γ</i> /deg	120	90	90
<i>V</i> /Å ³	3561(2)	5480.9(13)	2914(2)
<i>Z</i>	2	4	4
<i>D</i> _{calcd} /g cm ⁻³	1.492	1.277	1.191
<i>F</i> (000)	1536	2232	1104
<i>μ</i> /mm ⁻¹	4.371	1.063	0.081
<i>θ</i> range	2.52–25.39	1.66–25.20	1.88–25.70
<i>R</i> ₁ , <i>wR</i> ₂ (all data)	0.0866, 0.2385	0.0724, 0.1264	0.0912, 0.1401
GOF (<i>F</i> ²)	1.063	1.031	1.080

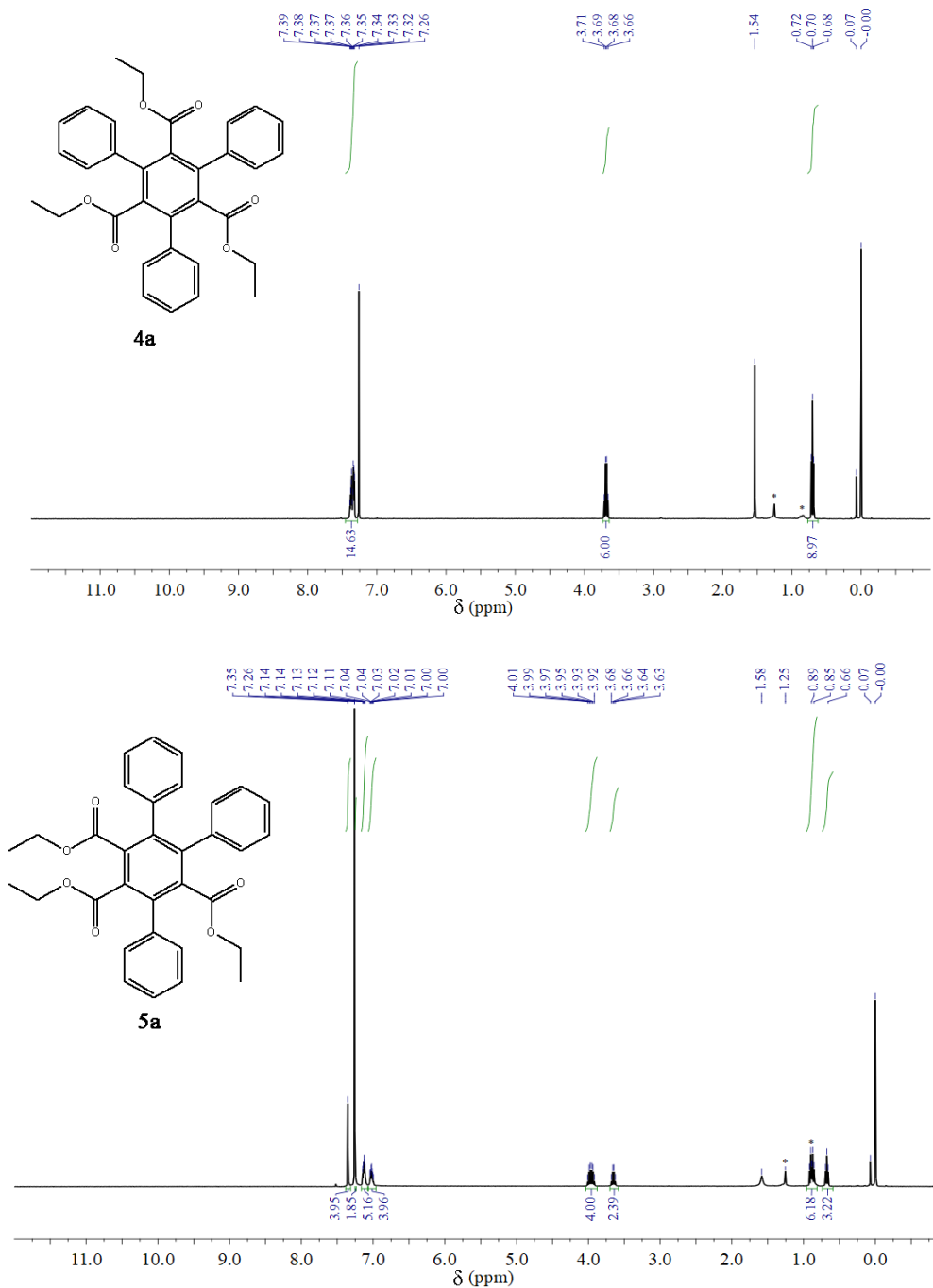
**Fig. S9.** X-ray structure of complex **4a** (30% probability level).

S1.3 Synthesis and characterization of the cyclotrimerization products

Synthesis and characterization of compounds **4a** and **5a**

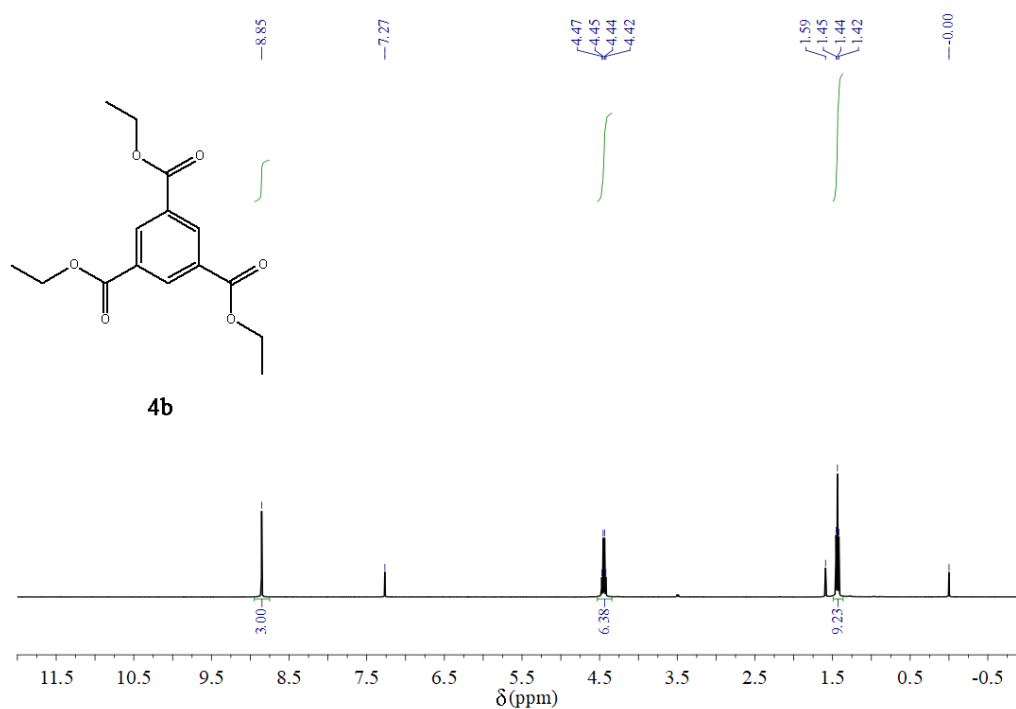
In a 15 mL sealed pressure tube were added ethyl phenylpropiolate (2.5 mmol, 0.436 g) and complex **2** with 5 mL of *n*-hexane, and the mixture was stirred at 100 °C for 5 h under Ar. After cooling to room temperature, the mixture was filtered and the precipitate was dissolved in CHCl₃. The pure products **4a** and **5a** were obtained by flash chromatography on silica gel (gradient of ethyl acetate/ petroleum ether = 1/20

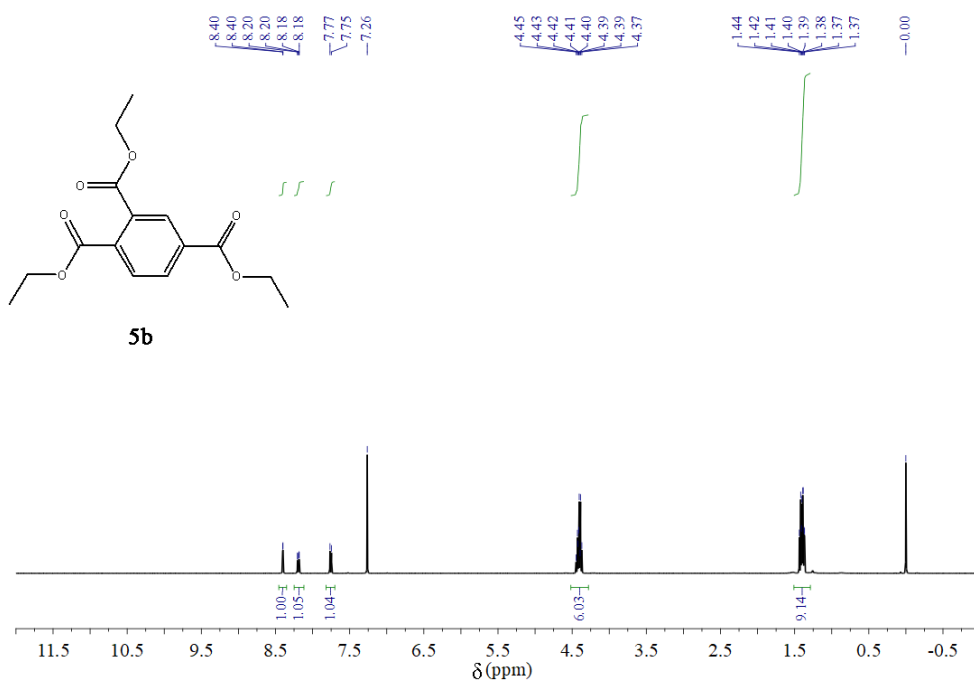
(v/v)). Compound **4a**:⁸ white solid, yield: 64% (0.280 g). M.p.: 212–214 °C. ¹H NMR (400 MHz, CDCl₃, TMS): δ = 7.39–7.32 (15H, m, Ar-*H*), 3.68 (6H, q, *J* = 7.2 Hz, CH₂), 0.70 (9H, t, *J* = 7.2 Hz, CH₃); IR (KBr/cm⁻¹) 2984(m), 1730 (v, ν_{C=O}), 1495(m), 1447(m), 1177(s), 1022(m), 760(m), 702(s). Compound **5a**:⁸ white solid, yield: 29% (0.126 g). M.p.: 151–153 °C. ¹H NMR (400 MHz, CDCl₃, TMS): δ = 7.35 (4H, s, Ar-*H*), 7.26 (2H, m, Ar-*H*), 7.13 (5H, m, Ar-*H*), 7.02 (4H, m, Ar-*H*), 3.96 (4H, m, CH₂), 3.65 (2H, q, *J* = 7.2 Hz, CH₂), 0.88 (6H, m, CH₃), 0.68 (2H, t, *J* = 7.2 Hz, CH₃). IR (KBr/cm⁻¹): 2981(m), 1731 and 1728 (s, ν_{C=O}), 1556(m), 1454(m), 1443(m), 1231(s), 1175(m), 1024(w), 764(w).



Synthesis and characterization of compounds **4b** and **5b**

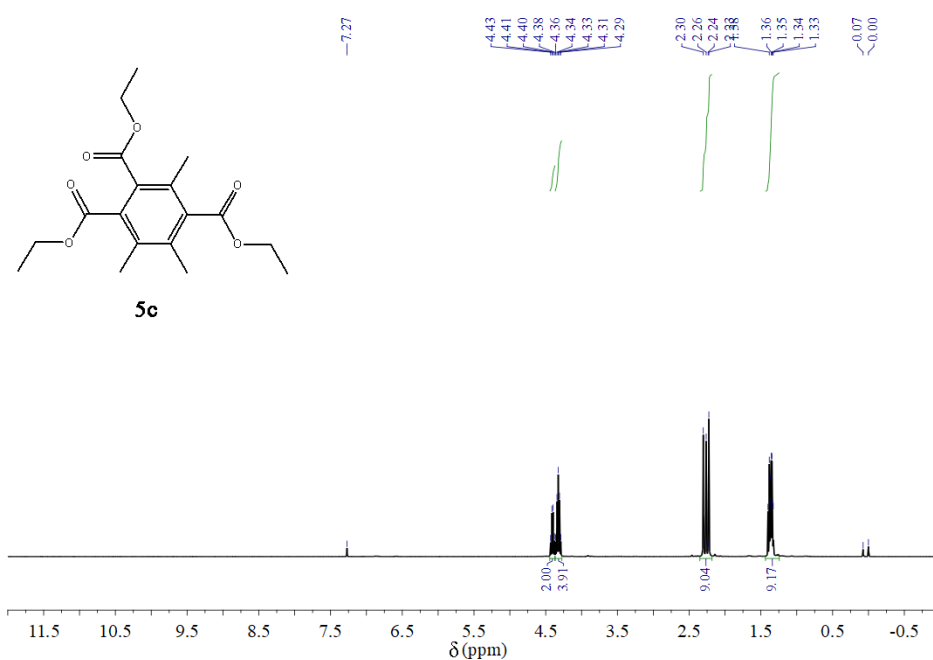
In a 15 mL sealed pressure tube were added ethyl propiolate (2.5 mmol, 0.245 g) and complex **2** with 5 mL of *n*-hexane, and the mixture was stirred at room temperature for 0.5 h under Ar. After standing overnight, the mixture was filtered, the filtrate concentrated, and the precipitate was collected. The crude product was recrystallized from *n*-hexane/ethyl acetate to afford a white solid of compound **4b**. The other product **4b** and **5b** were obtained from the filtrate by flash chromatography on silica gel (gradient of ethyl acetate/ petroleum ether = 1/10 (v/v)). Compound **4b**:⁹ white solid, yield: 55% (0.134 g). M.p.: 132–133 °C. ¹H NMR (400 MHz, CDCl₃, TMS): δ = 8.85 (1H, s, Ar-*H*), 4.45 (6H, m, CH₂), 1.44 (9H, t, *J* = 8.0 Hz, CH₃). IR (KBr/cm⁻¹): 2986(m), 1730(vs, ν_{C=O}), 1389(m), 1306(s), 1283(s), 1242(vs), 1113(s), 1067(s), 1022(s), 866(w), 795(w), 752(m). Compound **5b**:^{9,10} yellow oil, yield: 23% (0.056 g). ¹H NMR (400 MHz, CDCl₃, TMS): δ = 8.40 (1H, s, Ar-*H*), 8.19 (1H, d, *J* = 8.0 Hz, Ar-*H*), 7.76 (1H, d, *J* = 8.0 Hz, Ar-*H*), 4.40 (6H, m, CH₂), 1.39 (9H, m, CH₃). IR (KBr/cm⁻¹): 2993 (m), 2950(m), 1724 (vs, ν_{C=O}), 1442(m), 1390(m), 1248(s), 1103(m), 1024(s), 839(m), 739(m), 719(m).





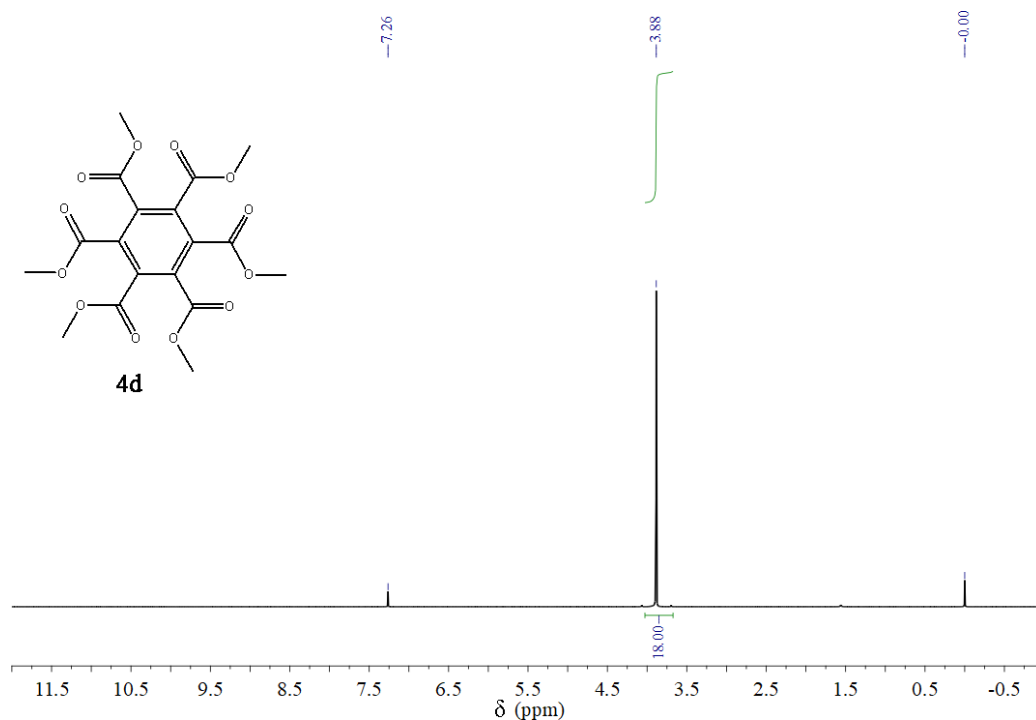
Synthesis and characterization of compound **5c**

In a 15 mL sealed pressure tube were added ethyl 2-butynoate (2.5 mmol, 0.280 g) and complex **2** with 5 mL of *n*-hexane, and the mixture was stirred at $100\text{ }^\circ\text{C}$ for 5 h under Ar. After cooling down, the volatiles were removed under reduced pressure and the pure product **5c** was obtained by flash chromatography on silica gel (gradient of ethyl acetate / petroleum ether = 1/10 (v/v)). Compound **5c**:¹⁰ yellow oil, yield: 78% (0.219 g). $^1\text{H NMR}$ (400 MHz , CDCl_3 , TMS): $\delta = 4.41$ (2H, q, $J = 8.0\text{ Hz}$, CH_2), $4.36\text{--}4.29$ (4H, q, $J = 8.0\text{ Hz}$, CH_2), 2.30 (3H, s, ArCH_3), 2.26 (3H, s, ArCH_3), 2.23 (3H, s, ArCH_3), $1.40\text{--}1.33$ (9H, m, CH_2CH_3); IR ($\text{KBr}/\text{cm}^{-1}$): $2986(\text{m})$, 1729 (vs, $\nu_{\text{C=O}}$), $1448(\text{m})$, $1418(\text{m})$, $1374(\text{m})$, $1320(\text{s})$, $1294(\text{s})$, $1214(\text{s})$, $1152(\text{s})$, $1037(\text{s})$, $850(\text{m})$, $797(\text{w})$, $718(\text{m})$.



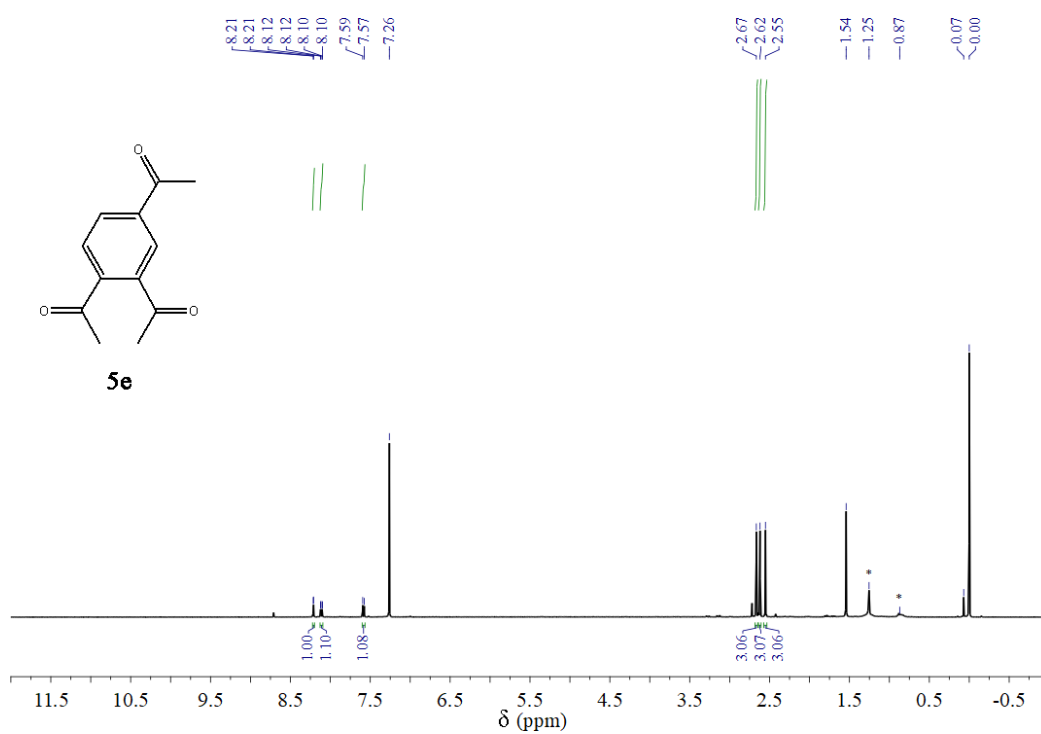
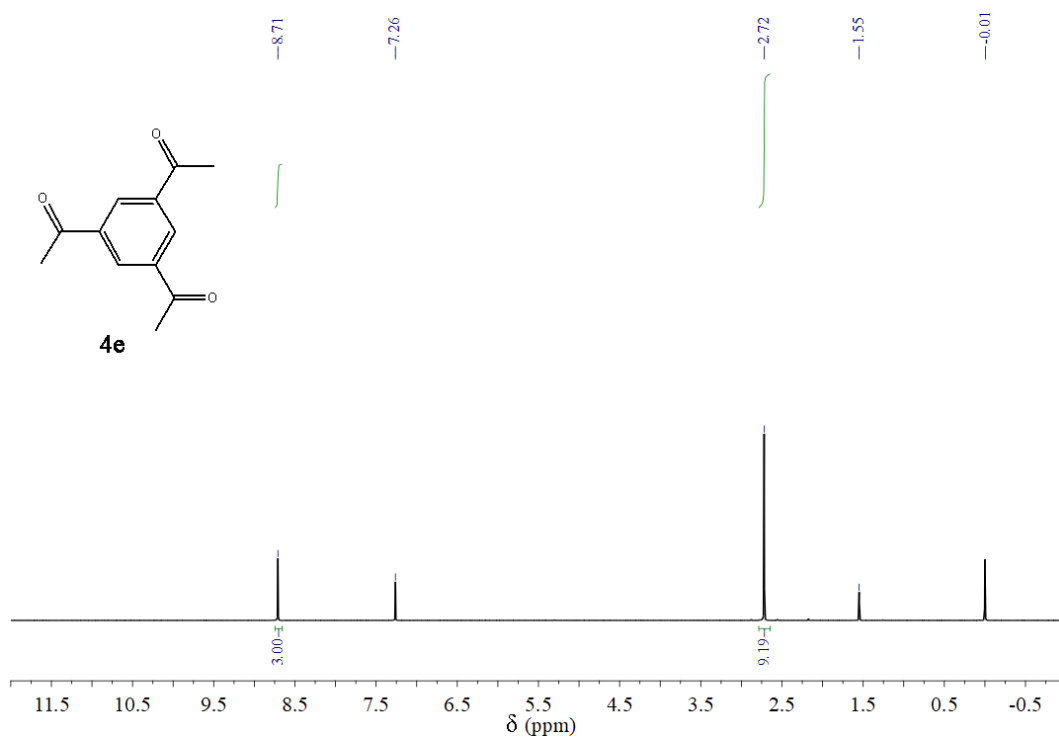
Synthesis and characterization of compounds 4d

In a 15 mL sealed pressure tube were added dimethyl but-2-ynedioate (2.5 mmol, 0.355 g) and complex **2** with 5 mL of *n*-hexane, and the mixture was stirred at room temperature for 0.5 h under Ar. The volatiles were removed under reduced pressure and the pure products **4d** were obtained by flash chromatography on silica gel (gradient of ethyl acetate / petroleum ether = 1/8 (v/v)). Compound **4d**:⁹ white solid, yield: 89% (0.316 g). M.p.: 189–190 °C. ¹H NMR (400 MHz, CDCl₃, TMS): 3.88 (18H, s, CH₃). IR (KBr/cm⁻¹): 3011(m), 2961(m), 1740(s, ν_{C=O}), 1445(s), 1414(m), 1364(s), 982(s), 856(s), 754(m)



Synthesis and characterization of compounds 4e and 5e

In a 15 mL sealed pressure tube were added dimethyl but-2-ynedioate (2.5 mmol, 0.170 g) and complex **2** with 5 mL of *n*-hexane, and the mixture was stirred at room temperature for 0.5 h under Ar. The volatiles were then removed under reduced pressure and the pure products **4e** and **5e** were obtained by flash chromatography on silica gel (gradient ethyl acetate / petroleum ether = 1/8 (v/v)). Compound **4e**:⁹ white solid, yield: 59% (0.101 g). M.p.: 156–157 °C. ¹H NMR (400 MHz, CDCl₃, TMS): 8.71 (3H, s, Ar-*H*), 2.72 (9H, s, CH₃). IR (KBr/cm⁻¹): 3086(w), 3062(m), 3003(m), 1690(vs, ν_{C=O}), 1585(m), 1420(m), 1362(s), 1227(s), 907(m), 687(m), 586(s). Compound **5e**:¹⁰ yellow oil, yield: 20% (0.034 g). ¹H NMR (400 MHz, CDCl₃): 8.21 (1H, s, Ar-*H*), 8.12 (1H, d, *J* = 8.0 Hz, Ar-*H*), 7.58 (1H, d, *J* = 8.0 Hz, Ar-*H*), 2.67 (3H, s, CH₃), 2.62 (3H, s, CH₃), 2.55 (3H, s, CH₃). IR (KBr/cm⁻¹): 3083(w), 3059(m), 1697 and 1700 (s, ν_{C=O}), 1601(m), 1424(m), 1355(s), 1235(s), 875(m), 867(m).

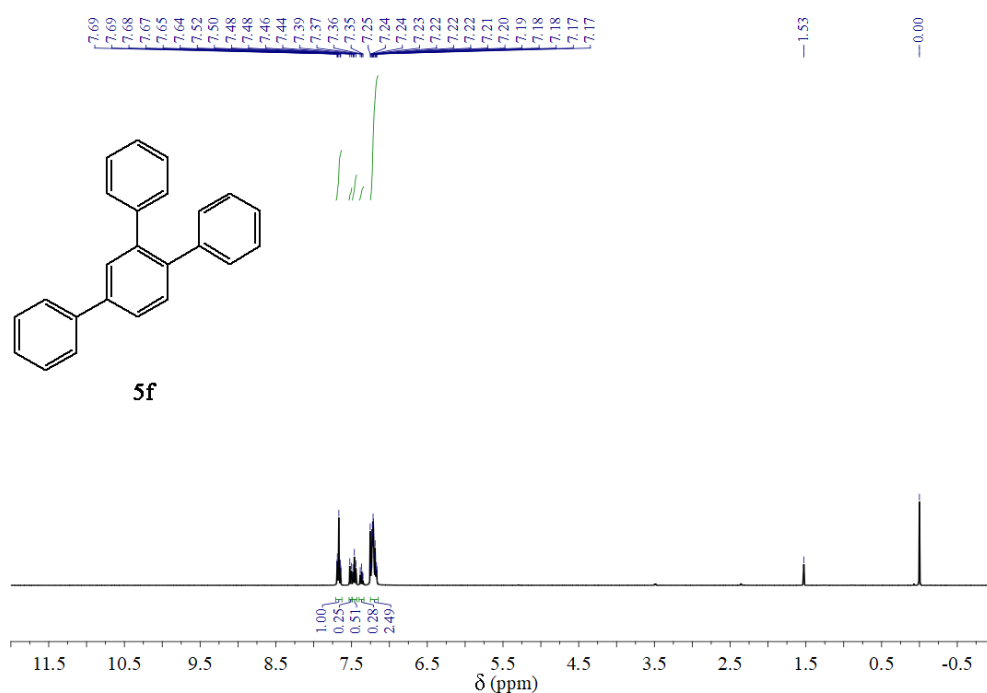
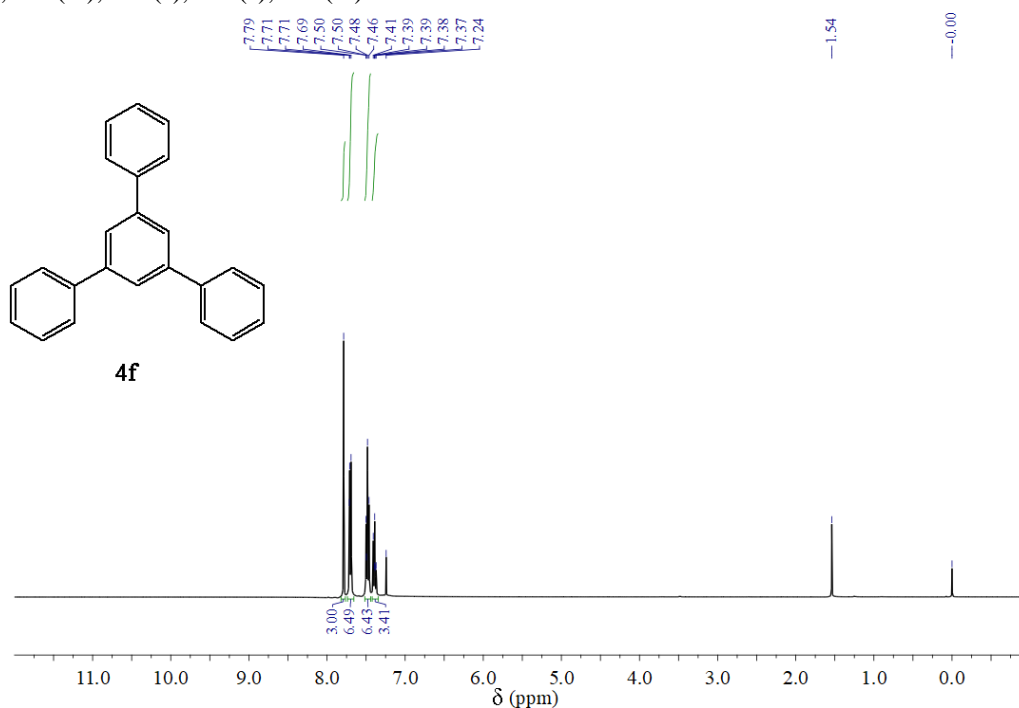


* peaks of solvent *n*-hexane.

Synthesis and characterization of compounds 4f and 5f

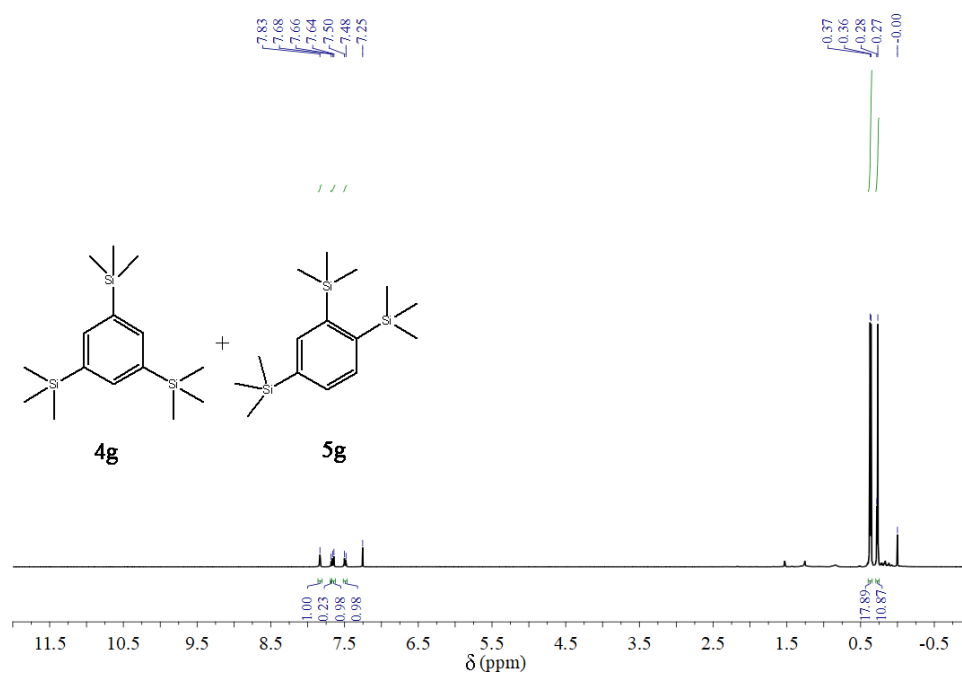
In a 15 mL sealed pressure tube were added phenylacetylene (2.5 mmol, 0.255 g) and complex **2** with 5 mL of *n*-hexane, and the mixture was stirred at 100 °C for 5 h under Ar. After cooling down, the volatiles

were removed under reduced pressure and the pure products **4f** and **5f** were obtained by flash chromatography on silica gel (eluent petroleum ether). Compound **4f**:⁹ white solid, yield: 42% (0.106 g). M.p.: 170–171 °C. ¹H NMR (400 MHz, CDCl₃, TMS): 7.79 (3H, s, C₆H₃, 1,3,5-(C₆H₅)₃C₆H₃), 7.70 (6H, d, *J* = 8.0 Hz, *o*-C₆H₅, 1,3,5-(C₆H₅)₃C₆H₃), 7.49 (6H, t, *J* = 8.0 Hz, *m*-C₆H₅, 1,3,5-(C₆H₅)₃C₆H₃), 7.40 (3H, t, *J* = 8.0 Hz, *p*-C₆H₅, 1,3,5-(C₆H₅)₃C₆H₃); IR (KBr/cm⁻¹): 3057(m), 1590(m), 1497(m), 1410(m), 872(m), 750(s), 690(s), 609(m). Compound **5f**:⁹ yellow solid, yield: 42% (0.106 g). M.p.: 115–117 °C. ¹H NMR (400 MHz, CDCl₃, TMS): 7.64–7.69 (4H, m, Ar-*H*), 7.51 (1H, d, *J* = 8.0 Hz, Ar-*H*), 7.48–7.44 (2H, m, Ar-*H*), 7.37 (1H, t, *J* = 8.0 Hz, Ar-*H*), 7.17–7.24 (10H, m, Ar-*H*). IR (KBr/cm⁻¹): 3061(m), 1600(m), 1477(s), 1439(s), 839(m), 764(s), 690(s), 573(m).



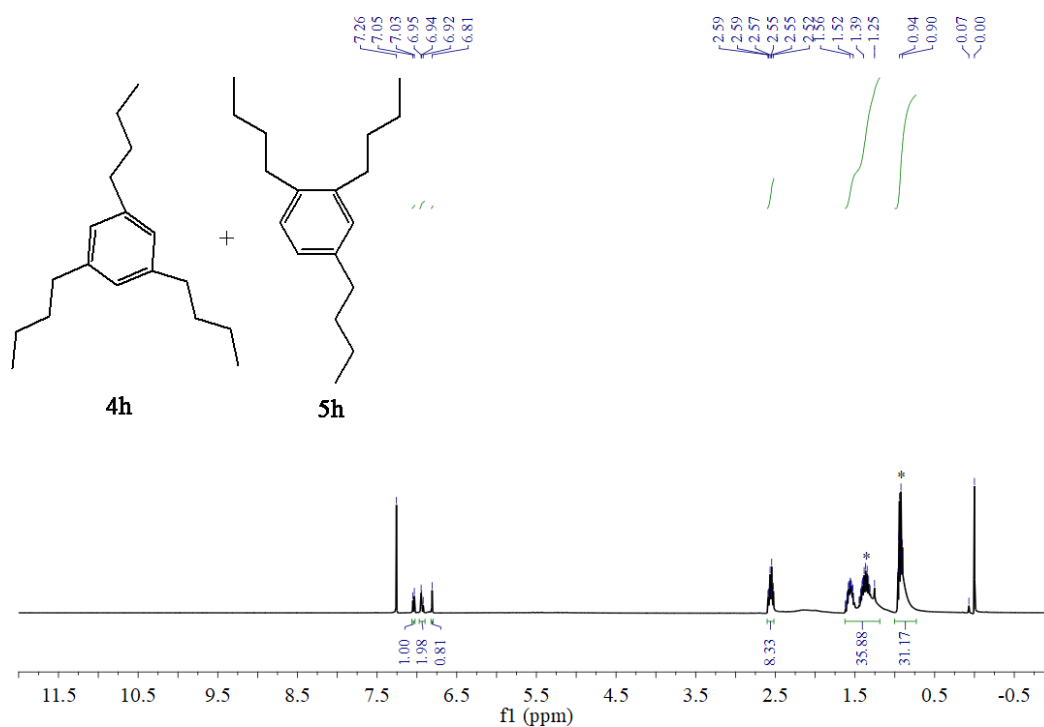
Synthesis and characterization of compounds **4g** and **5g**

In a 15 mL sealed pressure tube were added trimethylsilyl acetylene (2.5 mmol, 0.245 g) and complex **2** with 5 mL of *n*-hexane, and the mixture was stirred at 100 °C for 5 h under Ar. After cooling down, the volatiles were removed under reduced pressure and the products **4g** and **5g** were obtained by flash chromatography on silica gel (eluent petroleum ether). **4g** + **5g**:¹¹ yellow oil, yield: 52% (0.127 g). ¹H NMR (400 MHz, CDCl₃, TMS): δ = 7.68 (3H, s, Ar-*H*, **4g**), 0.28 (27H, s, Me₃Si, **4g**), 7.83 (1H, s, Ar-*H*, **5g**), 7.65 (1H, d, *J* = 8.0 Hz, Ar-*H*, **5g**), 7.49 (1H, d, *J* = 8.0 Hz, Ar-*H*, **5g**), 0.37 (9H, s, Me₃Si, **5g**), 0.36 (9H, s, Me₃Si, **5g**), 0.27 (9H, s, Me₃Si, **5g**).



Synthesis and characterization of compounds **4h** and **5h**

In a 15 mL sealed pressure tube were added 1-hexyne (2.5 mmol, 0.205 g) and complex **2** with 5 mL of *n*-hexane, and the mixture was stirred at 100 °C for 5 h under Ar. After cooling down, the volatiles were removed under reduced pressure and the products **4h** and **5h** were obtained by flash chromatography on silica gel (eluent petroleum ether). Compounds **4h** + **5h**:⁹ yellow oil, yield: 38% (0.078 g). ¹H NMR (400 MHz, CDCl₃, TMS): δ = 7.05–7.03 (1H, d, *J* = 7.6 Hz Ar-*H*, **5h**), 6.95–6.92 (2H, m, Ar-*H*, **5h**), 6.81 (1H, s, Ar-*H*, **4h**), 2.56 (8H, m, CH₂, **4h**+**5h**), 1.56 (8H, m, CH₂, **4h**+**5h**), 1.37 (8H, m, CH₂, **4h**+**5h**), 0.94 (11H, s, CH₃, **4h**+**5h**).



* peaks of solvent *n*-hexane.

S1.4 Kinetics studies

5 mM of complex 2: Complex **2** (21.0 mg, 0.020 mmol, 1 mol%) was placed in a Schlenk tube under an argon atmosphere and dissolved in dry *n*-hexane (4 mL). Portions (0.5 mL) of this solution were transferred to six sealed pressure tubes (10 mL) and ethyl phenylpropiolate (500 mM, 41 μ L, 0.25 mmol) was added to each tube and the mixture was stirred for 10, 20, 30, 40, 50 and 60 min, respectively, at 100 $^{\circ}$ C. The resulting solution was filtered and washed with chloroform (10 mL). After evaporating solvent, the crude residue was analyzed by 1 H NMR to determine the chemical yield, by the integration value of peaks at 4.27–4.32 ppm (**3a**: OCH_2CH_3) and peaks at 3.92–4.01 and 3.63–3.72 ppm (**4a** + **5a**: OCH_2CH_3).

10 mM complex 2: Following a same procedure, complex **2** (42.2 mg, 0.040 mmol, 2 mol%) and ethyl phenylpropiolate (500 mM, 41 μ L, 0.25 mmol) were used.

15 mM complex 2: Complex **2** (63.1 mg, 0.060 mmol, 3 mol%) and ethyl phenylpropiolate (500 mM, 41 μ L, 0.25 mmol) were used.

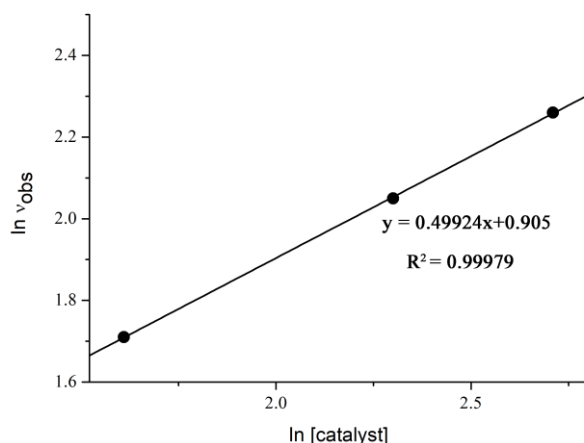
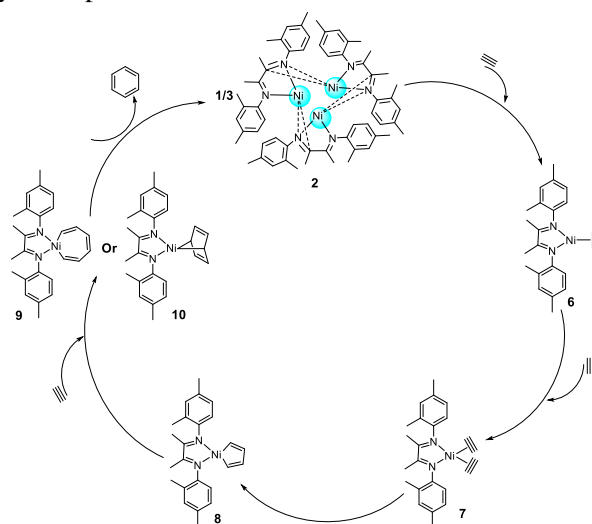


Fig. S10. Ln-Ln plot of observed rate constant vs. [catalyst] at 100 °C. By assuming pseudo first-order consumption of **3a** to give **4a** and **5a**, $\ln v_{\text{obs}}$ is plotted versus $\ln[\text{catalyst}]$, showing half-order dependency in concentration of the catalyst component.



Scheme S1. Proposed mechanism for the alkyne cyclotrimerization catalytic cycle of the complex **2**.

S2. DFT Computations

Computations for **2** were conducted using the bp86/6-311G(d) method¹² of the Gaussian 03 software package.¹³ Geometry optimization gave bond distances that are in good agreement with the X-ray structure.

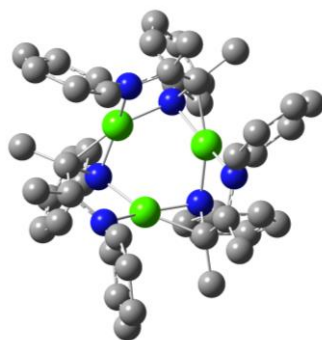


Fig. S11. Optimized structure of **2** (hydrogen atoms have been omitted for clarity).

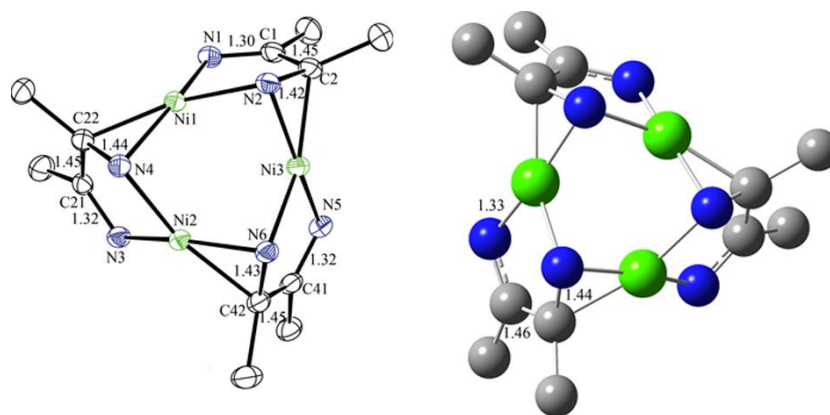


Fig. S12. Selected bond lengths of **2** (hydrogen atoms and the aryl rings are omitted for clarity).

Table S3. Cartesian coordinates of the optimized geometry of **2** in the singlet state.

Ni	1.53307500	0.42318300	0.25127600	H	-1.23629800	1.49207000	3.20543300
Ni	-0.40005100	-1.53927300	0.25127600	C	2.64304600	1.42004000	-2.22979800
Ni	-1.13302400	1.11609100	0.25127600	C	4.02498900	1.34531600	-1.96293800
N	0.39676100	1.79078600	1.07214200	C	4.93564600	1.08659700	-2.99170900
N	1.76110300	1.65685700	-1.14442400	H	6.00647600	1.04764500	-2.76782500
N	1.35248600	-1.23899900	1.07214200	C	4.48362600	0.87679800	-4.30422200
N	0.55432900	-2.35358800	-1.14442400	C	3.10954100	0.93013500	-4.57376200
N	-1.74924700	-0.55178800	1.07214200	H	2.74405700	0.75974500	-5.59170900
N	-2.31543100	0.69673100	-1.14442400	C	2.19286800	1.20048400	-3.54841200
C	-0.62935700	4.04002400	0.39575200	H	1.11945400	1.22942000	-3.75672800
H	0.12359700	4.82282400	0.61034000	C	3.81344200	-1.47497300	0.39575200
H	-1.26168500	3.94385500	1.28966900	H	4.11489000	-2.51845000	0.61034000
H	-1.26733000	4.40268400	-0.42513600	H	4.04632100	-0.87927600	1.28966900
C	0.00000000	2.70561800	0.03567000	H	4.44650100	-1.10380200	-0.42513600
C	0.84605500	2.62515000	-1.15286200	C	2.34313400	-1.35280900	0.03567000
C	0.69391700	3.64297200	-2.25095800	C	1.85042000	-2.04528000	-1.15286200
H	1.50044100	3.57986000	-2.99262600	C	2.80794800	-2.42243600	-2.25095800
H	0.69028400	4.66153000	-1.82930400	H	2.35002900	-3.08935000	-2.99262600
H	-0.26786200	3.51478700	-2.77687200	H	3.69186200	-2.92856800	-1.82930400
C	0.57950200	2.31853000	2.39026800	H	3.17782600	-1.52541800	-2.77687200
C	1.73190700	3.08451300	2.66463700	C	1.71815500	-1.66112900	2.39026800
C	1.94947300	3.60474500	3.94420300	C	1.80531300	-3.04213200	2.66463700
H	2.84835300	4.19830400	4.14144100	C	2.14706400	-3.49066500	3.94420300
C	1.02542100	3.36274300	4.97291100	H	2.21166100	-4.56589800	4.14144100
C	-0.11904000	2.60056800	4.70381900	C	2.39951000	-2.56941200	4.97291100
H	-0.84906600	2.40377500	5.49511000	C	2.31167700	-1.19719200	4.70381900
C	-0.34719100	2.08828400	3.41986300	H	2.50626300	-0.46657500	5.49511000

C	1.98210200	-0.74346600	3.41986300	C	-2.19263800	-1.40337500	4.70381900
H	1.91031900	0.32463000	3.20543300	H	-1.65719700	-1.93720000	5.49511000
C	-0.09173200	-2.99896500	-2.22979800	C	-1.63491200	-1.34481800	3.41986300
C	-0.84741700	-4.15840000	-1.96293800	H	-0.67402100	-1.81670000	3.20543300
C	-1.52680300	-4.81769300	-2.99170900	C	-2.55131400	1.57892500	-2.22979800
H	-2.09595000	-5.72558300	-2.76782500	C	-3.17757200	2.81308400	-1.96293800
C	-1.48248400	-4.32133300	-4.30422200	C	-3.40884300	3.73109600	-2.99170900
C	-0.74925000	-3.15800900	-4.57376200	H	-3.91052500	4.67793800	-2.76782500
H	-0.71407000	-2.75629500	-5.59170900	C	-3.00114200	3.44453600	-4.30422200
C	-0.05678400	-2.49932100	-3.54841200	C	-2.36029100	2.22787400	-4.57376200
H	0.50498200	-1.58418500	-3.75672800	H	-2.02998700	1.99655000	-5.59170900
C	-3.18408500	-2.56505100	0.39575200	C	-2.13608400	1.29883700	-3.54841200
H	-4.23848600	-2.30437400	0.61034000	H	-1.62443600	0.35476500	-3.75672800
H	-2.78463600	-3.06457800	1.28966900	H	-4.04158600	0.50358700	1.86098300
H	-3.17917100	-3.29888200	-0.42513600	H	-3.86055500	-0.84484200	5.97558200
C	-2.34313400	-1.35280900	0.03567000	H	1.58467400	-3.75191000	1.86098300
C	-2.69647400	-0.57987000	-1.15286200	H	2.66193200	-2.92091700	5.97558200
C	-3.50186500	-1.22053600	-2.25095800	H	-0.87711600	-4.53143700	-0.93526600
H	-3.85047000	-0.49051000	-2.99262600	H	-2.01930200	-4.83434000	-5.10763800
H	-4.38214500	-1.73296200	-1.82930400	H	-3.48578200	3.02532300	-0.93526600
H	-2.90996400	-1.98936900	-2.77687200	H	-3.17701000	4.16593700	-5.10763800
C	-2.29765700	-0.65740100	2.39026800	H	4.36289800	1.50611400	-0.93526600
C	-3.53722000	-0.04238100	2.66463700	H	5.19631200	0.66840300	-5.10763800
C	-4.09653700	-0.11408000	3.94420300	H	2.45691200	3.24832200	1.86098300
H	-5.06001500	0.36759400	4.14144100	H	1.19862200	3.76576000	5.97558200
C	-3.42493100	-0.79333100	4.97291100				

References

- (a) L. G. L. Ward, *Inorg. Synth.* 1972, **13**, 154. (b) A. A. Kestel-Jakob and G. Helmut, *Jordan J. of Chem.*, 2007, **2**, 219-233.
- (a) S. Bhattacharya, S. Sasmal, L. Carrella, E. Rentschler and Mohanta, *S. Dalton Trans.*, 2014, **43**, 12065–12076; (b) J. Jia, P. Ma, P. Zhang, D. Zhang, C. Zhang, J. Niu and J. Wang, *Dalton Trans.*, 2018, **47**, 6288–6292; (c) B. S. Bassil, Y. Xiang, A. Haider, J. Hurtado, G. Novitchi, A. K. Powell, A. M. Bossoh, I. M. Mbomekalle, P. Oliveira and U. Kortz, *Chem. Commun.*, 2016, **52**, 2601–2604; (d) M. Du, X. -H. Bu, Y. -M. Guo, L. Zhang, D. -Z. Liao and J. Ribasb, *Chem. Commun.*, 2002, 1478–1479;
- (a) A. P. Ginsberg, R. L. Martin and Sherwood, R. C. *Inor. Chem.*, 1968, **7**, 932–936.
(b) J. W. Zhao, J. Zhang, S. T. Zheng and G. Y. Yang, *Chem. – Eur. J.*, 2007, **13**, 10030.
- A. Klein, A. -K. Schmieder, N. Hurkes, C. Hamacher, A. O. Schüren, M. P. Feth and H. Bertagnolli, *Eur. J. Inorg. Chem.*, 2010, 934–941.

5. N. Altınölçek, M. Aydemir, M. Tavaslı, P. L. D. Santos and A. P. J. Monkman, *Organomet. Chem.*, 2017, **851**, 184–188.
6. G. M. Sheldrick, *Program SADABS: Area-Detector Absorption Correction*; University of Göttingen, Germany, 1996.
7. G. M. Sheldrick, *SHELXS-97 and SHELXL-97, Programs for Crystal Structure Analysis*; University of Göttingen, Germany, 1997.
8. R. Diercks and H. tom Dieck, *Z. Naturforsch.*, 1984, **39b**, 180–184;
9. V. Cadierno, J. Francos, S. E. García-Garrido and J. Gimeno, *J. Green Chem. Lett. Rev.* 2011, **4**, 55–61.
10. S. K. Rodrigo, I. V. Powell, M. G. Coleman, J. A. Krause and H. Guan, *Org. Biomol. Chem.* 2013, **11**, 7653–7657.
11. G. Hilt, T. Vogler, W. Hess and F. Galbiati, *Chem. Commun.*, 2005, 1474–1475.
12. (a) A. D. Becke, *Phys. Rev. A*, 1988, **38**, 3098; (b) J. P. Perdew, *Phys. Rev. B*, 1986, **33**, 8822; *erratum*: J. P. Perdew, *Phys. Rev. B*, 1986, **34**, 7406.
13. M. J. Frisch, G. W. Trucks, H. B. Schlegel, G. E. Scuseria, M. A. Robb, J. R. Cheeseman, J. A. Montgomery, J. T. Vreven, K. N. Kudin, J. C. Burant, J. M. Millam, S. S. Iyengar, J. Tomasi, V. Barone, B. Mennucci, M. Cossi, G. Scalmani, N. Rega, G. A. Petersson, H. Nakatsuji, M. Hada, M. Ehara, K. Toyota, R. Fukuda, J. Hasegawa, M. Ishida, T. Nakajima, Y. Honda, O. Kitao, H. Nakai, M. Klene, X. Li, J. E. Knox, H. P. Hratchian, J. B. Cross, V. Bakken, C. Adamo, J. Jaramillo, R. Gomperts, R. E. Stratmann, O. Yazyev, A. J. Austin, R. Cammi, C. Pomelli, J. W. Ochterski, P. Y. Ayala, K. Morokuma, G. A. Voth, P. Salvador, J. J. Dannenberg, V. G. Zakrzewski, S. Dapprich, A. D. Daniels, M. C. Strain, O. Farkas, D. K. Malick, A. D. Rabuck, K. Raghavachari, J. B. Foresman, J. V. Ortiz, Q. Cui, A. G. Baboul, S. Clifford, J. Cioslowski, B. B. Stefanov, G. Liu,; A. Liashenko, P. Piskorz, I. Komaromi, R. L. Martin, D. J. Fox, T. Keith, M. A. Al-Laham, C. Y. Peng, A. Nanayakkara, M. Challacombe, P. M. W. Gill, B. Johnson, W. Chen, M. W. Wong, C. Gonzalez, J. A. Pople, Gaussian 03, Revision E.01, Gaussian, Inc., Wallingford CT, 2004.